ImmunoHorizons, 2026, **10**(3), vlag001
https://doi.org/10.1093/immhor/vlag001
Research Article | Clinical and Translational Immunology

Phenotypically similar but functionally distinct NK cell populations within the human maternal-fetal interface

Marie Frutoso[1,4], Caitlin S. DeJong[1], Raj Shree[2], Stephen A. McCartney[2], and Martin Prlic[1,3,*]

[1]Vaccine and Infectious Disease Division, Fred Hutchinson Cancer Center, Seattle, WA, United States
[2]Division of Maternal Fetal Medicine, Department of Obstetrics and Gynecology, University of Washington, Seattle, WA, United States
[3]Department of Global Health, University of Washington, Seattle, WA, United States
[4]Present address: LBAI, UMR1227, Univ Brest, Inserm, Brest, France
*Corresponding author: Vaccine and Infectious Disease Division, Fred Hutchinson Cancer Center, 98109 Seattle, WA, United States.
Email: mprlic@fredhutch.org

Abstract

Natural killer (NK) cell function within tissues extends beyond exerting cytotoxicity, encompassing a range of functions that are just starting to become fully elucidated. In the context of human placentation, NK cells play a key role in enabling initial placentation, which is associated with the acquisition of tolerance-like properties. If and to which extent NK cells maintain these tolerance-like properties over the course of human pregnancy is still poorly understood. We asked if NK cells isolated from the decidual-placental interface of full-term human pregnancies are able to exert effector function. We observed a significant and striking lack in the ability of NK cells isolated from the decidual-placental interface (DPI) to produce interferon-g (IFN-γ) in response to the activating cytokines interleukin (IL)-12, IL-15, and IL-18. In contrast, NK cells from the decidua retained their responsiveness to cytokine-mediated activation. Notably, $CD103^{+}CD69^{+}$ tissue-resident NK cells were present in both DPI and decidua, yet exhibited distinct effector function from one another. Using high-parameter flow cytometry and single-cell sequencing, we found that this functional discrepancy was not directly predictable based on their cell surface phenotype or cell transcript. Together, our findings reveal the presence of distinct functional resident NK cell populations in 2 anatomically adjacent tissues at healthy full-term pregnancies.

Keywords NK cells, tissue residency, function, high-parameter flow cytometry, single-cell transcriptomics

Introduction

Natural killer (NK) cells are an important component of the immune system and play a key role in fighting infections and tumors.[1–5] NK cells are located both in blood and tissues [6,7] and their function within tissues extends beyond cytotoxicity. NK cells can either foster inflammation and attract dendritic cells (DC) [8,9] or, conversely, mitigate inflammation by aiding in the removal of adaptive immune cells, such as CD4 via the TRAIL-dependent pathway,[10–12] or in a perforin-dependent manner [13,14] or through the secretion of IL-10.[15,16] NK cell functional adaptability can be further appreciated in the context of placentation. During the first trimester, NK cells adopt tolerogenic properties, facilitating the implantation of fetal cells in the endometrium.[17,18] During the first trimester of pregnancy, NK cells account for over 70% of the immune cells within the decidua and exert key roles for pregnancy success facilitating implantation, spiral artery remodeling, trophoblast invasion, and immunity to infection.[19–21] At term, NK cells persist with reduced relative frequency due to an increase of T cells.[22–25] Importantly, whether these tolerogenic NK cell properties from the first trimester are maintained during the entire pregnancy or change over time is unclear. The interface between the placenta and decidua changes over the course of the pregnancy, consisting of heterogeneous tissue comprised of both maternal- and fetal-derived cells.[17] Most of the placenta contains fetal-derived cells including the syncytiotrophoblast, cytotrophoblasts, endothelial, Hofbauer, and stromal cells. These cells are involved in nutrient and gas exchange with maternal blood, maintenance of the placental structure, and possess a role in immune regulation and tissue remodeling.[26–28] Maternal-derived immune and stromal cells are found in the decidua, the lining of the uterus during pregnancy. We refer to the tissue interface of placenta and decidua as the decidual-placental interface (DPI). Although the maternal and fetal-derived structures of the placenta can be clearly distinguished by histology, maternal immune cells present in the DPI can interact with or at the very least be exposed to signals from both maternal and fetal cells.

We asked if NK cells that are present in the DPI are able to respond to pro-inflammatory signals and found that DPI NK cells had a decreased ability to produce inflammatory cytokines in response to stimulation in comparison to decidual NK cells

Received: October 3, 2025. **Revised:** December 29, 2025. **Accepted:** January 5, 2026

(farther away from fetal-derived cells). This functional discrepancy of NK cells based on tissue location was not apparent from phenotyping NK cells by flow cytometry or single-cell RNAseq: NK cells from the DPI and decidua appeared to have rather congruent phenotypic and transcriptional profile. Our data indicate the presence of phenotypically similar but functionally distinct resident NK cell populations within the full-term maternal-fetal interface.

Material and methods

Study population and approvals

We obtained samples (placenta, decidua, and matched-peripheral blood) from heathy pregnant individuals at the University of Washington Medical Center (Seattle, Washington, USA) under Institutional Review Board (IRB) approved studies from the University of Washington (STUDY00001636). All individual participants gave written informed consent prior to participation. We included pregnant individuals >18 yr old with non-anomalous singleton fetus undergoing a scheduled cesarean delivery at term gestation (between 37 and 41 wks gestation). Individuals with pregnancy complications including multiple gestation, pre- or gestational diabetes, preeclampsia, preterm labor, or placental abnormalities were excluded. Cryopreserved peripheral blood mononuclear cells (PBMCs) from healthy controls were used as a longitudinal technical control for all flow cytometry acquisitions.

Isolation of leukocytes from tissues and peripheral blood

After surgical procedures, fresh tissue samples were maintained on ice and samples were processed within 1–4 h after collection. Maternal peripheral blood (mBlood) was collected prior to delivery in ACD tubes and then processed using SepMate tubes (StemCell Technologies, 85450) and Lymphoprep (Stem Cell Technologies, 07851) according to manufacturer protocols.

To obtain decidual tissue, residual tissue in the uterine cavity was vacuum aspirated.[29] Placentas were rinsed in 1× PBS and sterile instruments were used to collect 0.5 cm-depth biopsies from the maternal-facing and fetal-facing sides of the placenta (DPI and ffPLAC, respectively). Decidual, DPI, and ffPLAC tissues were minced and incubated at 37 °C with Collagenase Type II (Sigma Aldrich) and 200U/ml DNase (Sigma Aldrich) in RPMI1640 with 7.5% FBS under agitation for 60 min at 225 RPM. Subsequently, any remaining tissue pieces were strained through a 70 μm filter, centrifuged cells at 400 g for 5 min, supernatants were discarded, and cells were washed with RPMI1640 with 7.5% FBS. Red blood cells were removed using ACK lysis, and cell pellets were resuspended in RPMI1640 with 7.5% FBS before downstream use.

Flow cytometry and cell sorting

Flow cytometric analysis was carried out directly after cell isolation (without cryopreservation) as previously described[30] and consensus suggestions for data analysis.[31] A detailed list of the main panels used, including fluorochromes, antibody catalogue numbers and final dilutions is provided in **Table 1**. Single-stained controls were prepared with every experiment using antibody capture beads (BD Biosciences anti-mouse (552843) or anti-mouse Plus, and anti-rat (552844)) and anti-REA (Miltenyi 130-104-693) diluted in FACS buffer, or cells for Live/Dead reagent, and treated exactly the same as the samples (including fixation procedures). For each staining of experimental samples, a PBMC sample from the same healthy donor was stained with the same panel as a technical reference control.

All samples were acquired using a FACSymphony A5 (BD Biosciences) as previously described.[32] Detector voltages were optimized using a modified voltage titration approach[33] and standardized from day to day using MFI target values and 6-peak Ultra Rainbow Beads [34] (Spherotec, URCP-38-2K). After acquisition, data was exported in FCS 3.1 format and analysed using FlowJo (version 10.6.x, and 10.7.x, BD Biosciences). Samples were analyzed using manual gating (**Fig. S1A**). Cell sorting was performed on cryopreserved samples either on a FACSAria III (BD Biosciences), equipped with 20 detectors and 405 nm, 488 nm, 532 nm, and 628 nm lasers or on a FACSymphony S6 cell sorter (BD Biosciences), equipped with 50 detectors and 355 nm, 405 nm, 488 nm, 532 nm and 628 nm lasers. A 70-μm nozzle at 70 psi sheath pressure was used. Unless stated otherwise, cells were sorted into chilled Eppendorf tubes containing 500–1,000 μl complete RPMI, washed once in PBS and immediately used for subsequent processing.

Ex vivo stimulation assays

Cells were isolated from tissues or blood as described above. Directly after isolation (without cryopreservation), 500,000 cells were placed into each well of a U-bottom 96-well plate with 200 μl complete media. Cells were then stimulated with IL-12, IL-15 and IL-18 (each at 1 nM) for 24hrs. GolgiPlug was added after 20hrs of culture.

Bulk RNA-seq experiments and analysis

Bulk RNA-seq was performed on 500 sort-purified NK cells from the mBlood ($n = 6$), the DPI ($n = 8$) or the decidua ($n = 6$) of 6 matched-donors and 2 additional donors for the DPI.

After thawing, Live, CD45+CD14-CD19-CD3-CD127-NKp46+ NK cells were sorted on a FACSAria III equipped with a 70um nozzle directly into lysis buffer from the SMART-Seq v4 Ultra Low Input RNA Kit for sequencing (Takara), immediately snap frozen on dry ice, and transferred to −80 °C storage until processed into cDNA. Subsequent processing occurred as previously described.[35] For differential gene expression comparisons, genes with a false discovery rate (FDR) of less than 0.1 and an absolute expression fold-change greater than 1 were considered differentially expressed.

Whole-transcriptome single-cell library preparation and sequencing

The cDNA libraries were generated using the BD Rhapsody™ system pipeline to generate libraries for Whole Transcriptome

Table 1. Antibodies used in the 27-color flow cytometry panel.

Specificity	Clone	Fluorochrome	Vendor	Catalog number	Titration
Dead cells	UV	Blue	eBiosciences	L23105	1:500
CD45	HI30	BUV805	BD Biosciences	564914	1:80
CD14	M5E2	BV570	BioLegend	301832	1:20
CD19	SJ250-C1	BUV395	BD Biosciences	563549	1:40
CD3	UCHT1	BUV661	BD Biosciences	565065	1:80
CD127	HIL-7R-M21	BV786	BD Biosciences	563324	1:10
HLA-DR	G46.6	APC-H7	BD Biosciences	641393	1:40
CD16	3G8	BUV496	BD Biosciences	564653	1:40
NKp46	9E2	Biotin	BioLegend	331906	1:640
Streptavidin		BB630	BD Biosciences custom antibody	624294	1:500
NKG2D	1D11	PE-Cy7	BD Biosciences	562365	1:5
CD244	2-69	BV421	BD Biosciences	565750	1:5
CD2	RPA-2.10	BV605	BioLegend	300224	1:160
NKG2A	REA110	PE	Miltenyi	130-113-566	1:160
CD161	DX12	BB700	BD Biosciences	745791	1:20
TIGIT	741182	BV711	BD Biosciences	747839	1:80
CD69	FN50	BV650	BioLegend	310933	1:20
CD39	TU66	PE-CF594	BD Biosciences	563678	1:160
CD57	NK-1	FITC	BD Biosciences	555619	1:80
CD27	M-T271	BB660	BD Biosciences custom antibody	624295	1:160
CD11b	ICRF44	PE-Cy5	BD Biosciences	555389	1:10
CD38	HIT2	BB-790-P	BD Biosciences custom antibody	624896	1:80
CX3CR1	2A9-1	BUV737	BD Biosciences	749355	1:40
CD103	Ber-ACT8	BV750	BD Biosciences	747099	1:160
Ki67	Sola15	eFluor660	eBiosciences	50-5698-80	1:1000
Granzyme B	QA16A2	AF700	BioLegend	372222	1:160
CD25	2A3	BUV563	BD Biosciences	565699	1:40
CD56	CMSSB	PECy5.5	ThermoFisher	35-0567-41	1:20

Analysis (WTA), AbSeq, and Sample Tag as previously described.[30] In brief, after thawing, cells from mBlood, CordBlood, DPI and Decidua were stained with a cytometry panel and one specific Sample-Tag for multiplexing (BD Biosciences SMK). Live, CD45+ cells were sorted after sorting, cells from all donors and tissues were pooled and stained with 58 oligo-antibodies. Stained cells were then loaded on the BD Rhapsody cartridges (between 35–45,000 cells were loaded per cartridges). The list of Abseq is available in **Table 2**. Final libraries were diluted to 3 nM and multiplexed for paired-end (100 bp) sequencing on a NovaSeq 6000 (Illumina) using S1 and S2 flow cells. For the gene expression library, we targeted 34,000—37,000 reads per cell, for the AbSeq library 22,000 reads per cell, and for the Sample-Tag libraries 2,000 reads per cell.

Pre-processing for whole transcriptome analysis (WTA) data

Fastq files were processed via the standard Rhapsody analysis pipeline (BD Biosciences) on Seven Bridges (www.sevenbridges.com). In brief, after read filtering, reads are aligned to a reference genome and annotated, barcodes and UMIs are counted, followed by determining putative cells. The final output (molecule per cell count matrix) was analysed in R using Seurat[36] (version 4.4.3) as previously described.[30] For the SMART-Seq v4 experiments, Fastq files were aligned to the GRCh38 reference genome as described in more detail above. Principal component analysis was used to generate 75 principal components, followed by data integration using Harmony.[37] The dimensionality reduction from Harmony was used for subsequent UMAP calculation and graph-based clustering with tuned resolution. Protein phenotyping data was stored in a separate slot as described in the Seurat tutorial for CITE-seq data, and normalized using the centered log ratio (CLR) method.[38] For all differential gene expression analyses we utilized the Seurat implementation of MAST (model-based analysis of single-cell transcriptomes) with the number of UMIs included as a covariate (proxy for cellular detection rate [CDR]) in the model.[39]

Statistical analyses

Unless stated otherwise, all data are represented as mean± SD. Statistical analyses between mblood, ffPLAC, DPI and decidua

Table 2. List of Oligo Antibodies used for Abseq.

Antibody	Clone	Provider	Category number
CD3	UCHT1	BD Biosciences	Abseq Immune Discovery Panel no. 625970
CD4	SK3	BD Biosciences	Abseq Immune Discovery Panel no. 625970
CD8	SK1	BD Biosciences	Abseq Immune Discovery Panel no. 625970
CD19	SJ25-C1	BD Biosciences	Abseq Immune Discovery Panel no. 625970
CD278 (ICOS)	DX29	BD Biosciences	Abseq Immune Discovery Panel no. 625970
CD127	HIL-7R-M21	BD Biosciences	Abseq Immune Discovery Panel no. 625970
CD28	L293	BD Biosciences	Abseq Immune Discovery Panel no. 625970
CD25	2A3	BD Biosciences	Abseq Immune Discovery Panel no. 625970
OX40	ACT35	BD Biosciences	Abseq Immune Discovery Panel no. 625970
CD45RA	HI100	BD Biosciences	Abseq Immune Discovery Panel no. 625970
Tim3	7D3	BD Biosciences	Abseq Immune Discovery Panel no. 625970
PD1	EH12.1	BD Biosciences	Abseq Immune Discovery Panel no. 625970
CD137	4B4-1	BD Biosciences	Abseq Immune Discovery Panel no. 625970
CD197 (CCR7)	2L1-A	BD Biosciences	Abseq Immune Discovery Panel no. 625970
CD161	HP-3G10	BD Biosciences	Abseq Immune Discovery Panel no. 625970
CD27	M-T271	BD Biosciences	Abseq Immune Discovery Panel no. 625970
CD56	NCAM16.2	BD Biosciences	Abseq Immune Discovery Panel no. 625970
CD196 (CCR6)	11A9	BD Biosciences	Abseq Immune Discovery Panel no. 625970
CD183 (CXCR3)	1C6-CXCR3	BD Biosciences	Abseq Immune Discovery Panel no. 625970
CD186 (CXCR6)	13B1E5	BD Biosciences	Abseq Immune Discovery Panel no. 625970
CD62L	DREG-56	BD Biosciences	Abseq Immune Discovery Panel no. 625970
CD134	ACT35	BD Biosciences	Abseq Immune Discovery Panel no. 625970
CD185 (CXCR5)	RF8B2	BD Biosciences	Abseq Immune Discovery Panel no. 625970
CD272	J168-540	BD Biosciences	Abseq Immune Discovery Panel no. 625970
CD357 (GITR)	V27-580	BD Biosciences	Abseq Immune Discovery Panel no. 625970
IgM	G20-127	BD Biosciences	Abseq Immune Discovery Panel no. 625970
IgD	IA6-2	BD Biosciences	Abseq Immune Discovery Panel no. 625970
CD14	MφP9	BD Biosciences	Abseq Immune Discovery Panel # no. 625970
CD16	3G8	BD Biosciences	Abseq Immune Discovery Panel no. 625970
CD11c	B-ly6	BD Biosciences	Abseq Immune Discovery Panel no. 625970
HLA-DR	G46-6	BD Biosciences	Abseq Immune Discovery Panel no. 625970
CD69	FN50	BD Biosciences	No. 940019
CD103	Ber-ACT8	BD Biosciences	No. 940067
CD45RO	UCHL1	BD Biosciences	No. 940022
CD38	HIT2	BD Biosciences	No. 940013
Lag3	T47-530	BD Biosciences	No. 940080
TCRgd	11F2	BD Biosciences	No. 940057
CD5	UCTH2	BD Biosciences	No. 940038
CD39	TU66	BD Biosciences	No. 970073
CD195 (CCR5)	3A9	BD Biosciences	No. 940050
CD194 (CCR4)	1G1	BD Biosciences	No. 940047
CD244	2-69	BD Biosciences	No. 940362
NKp46	9E2/nkp46	BD Biosciences	No. 940064
CD11b	M1-70	BD Biosciences	No. 940008
CD141	1A4	BD Biosciences	No. 940079
CD1c	F10/21A3	BD Biosciences	No. 940083
CD123	7G3	BD Biosciences	No. 940020
CD40	5C3	BD Biosciences	No. 940049
CD86	FUN-1	BD Biosciences	No. 940025
CD80	L307.4	BD Biosciences	No. 940036
CD206	19.2	BD Biosciences	No. 940068
CD32	FLI8.26	BD Biosciences	No. 940069
CD163	GHI/61	BD Biosciences	No. 940058

(continued)

Table 2. (continued)

Antibody	Clone	Provider	Category number
CD274	MIH1	BD Biosciences	No. 940035
CX3CR1	2A9-1	BD Biosciences	No. 940216
CCR2	1D9	BD Biosciences	No. 940286
VISTA	MIH65.rMAb	BD Biosciences	No. 940497
CD117 ckit	104D2	BD Biosciences	No. 940250

samples were performed using one-way ANOVA with Tukey's multiple comparisons test. *P*-values are shown in full, except if smaller than 0.0001. Statistical analysis was performed using GraphPad Prism (v9).

Immunofluorescence

The image of the DPI was generated in collaboration with Miltenyi Biotec using the MACSima™ Platform and MACS® iQ View Analysis Software.

Results

Functionally distinct NK cells in the decidua versus decidual-placental interface

In present-day obstetrics, cesarean delivery (C-section) account for approximately 20% of all childbirths (https://www.who.int/news/item/16-06-2021-caesarean-section-rates-continue-to-rise-amid-growing-inequalities-in-access). During the surgery, the placenta is removed and, for this study, the uterine cavity was aspirated in order to remove any remaining membranes and decidual tissue. We collected both placental tissue (containing the basal plate) and the remaining decidual tissues from healthy, unlabored pregnancies (**Fig. 1A and B**). We first asked if the spatial proximity of NK cells to fetal-derived tissue results in any changes of their functional properties. We distinguished 3 different tissue zones: a fetal-facing side of the placenta (ffPLAC), the decidual-placental interface (DPI) which includes both decidual basalis as well as placental villi, and the remaining aspirated decidua (containing maternal-derived cells that are more distal from the placenta). Of note, NK cells from the ffPLAC, primarily consisting of the chorionic plate, are likely to be of fetal origin or from the maternal blood and were included as a reference population. We biopsied sections of 0.5 cm depth for each zone, isolated cells using enzymatic digestion and verified by flow cytometry that NK cells were present in all tissues (**Figs. 1C and S1A**). The frequency of NK cells was similarly increased in the DPI and the Decidua compared to the maternal peripheral blood (mBlood) and the ffPLAC (although not significant for the latter).

To determine if the different tissue sites are associated with distinct NK cell functionality, we assessed NK cell response to ex vivo stimulation with pro-inflammatory cytokines. We specifically stimulated with IL-12, IL-15, and IL-18; 3 cytokines associated with inflammation that play key roles in NK cell biology,[40–46] and measured the production of IFN-γ, a key effector molecule.[1,47] NK cells from the DPI showed a significantly decreased ability to produce IFN-γ in response to stimulation compared to NK cells from the mBlood, the decidua, and the ffPLAC (**Fig. 1D**).

Functionally distinct resident NK cells after stimulation

We next asked if this difference in function was associated with distinct tissue-associated phenotypes. Resident uterine NK cells from the first trimester possess impaired effector function.[22,26,48,49] In particular, the interaction of non-polymorphic HLA-E and HLA-G molecules with their respective receptors CD94/NKG2 and KIR2DL4 on the surface of NK cells has been shown to decrease their cytotoxicity.[50] However, this interaction was shown to increase IFN-γ secretion during the 1st trimester.[50] Other receptors of NK cells, activating or inhibitory could modulate NK cell function and contribute to distinct NK cells subtypes.[51] To assess biomarkers indicative of tissue residence and activation, we used a previously developed panel of 27-marker to interrogate the NK cell profile within tissues.[32] The panel included resident, maturation, activation, activating and inhibitory receptors which could indicate distinct NK cell functional subsets. We first utilized dimensionality reduction using uniform manifold approximation projections (UMAP) on pre-gated NK cells for unsupervised analysis of NK cell phenotype. We observed a cluster of NK cells specific to the decidua and the DPI (**Fig. 2A**). This cluster differed from the rest of the NK cells by the concomitant expression of the established residency markers CD103 and CD69[6,52–58] as well as the lack of expression of CD16 and CD57 as typically observed on mature NK cells[59,60] (**Fig. 2B**). We next manually gated on these populations to further examine their phenotype and observed a significant increase in CD103 and CD69 expression in the DPI and the decidua in comparison to the mBlood and the ffPLAC. The increase was associated with the decreased expression of CD16 in NK cells from the DPI and the decidua compared to circulating NK cells and NK cells from the ffPLAC (**Fig. 2C**). As residency can affect NK cell functionality,[6,61–65] we looked at IFN-γ production by CD103$^+$ or CD103$^-$ NK cells. Unexpectedly, we saw a similar decrease of IFN-γ production by NK cells from both CD103$^-$ and CD103$^+$ NK cell subsets in the DPI compared to the decidua. In the mBlood and the ffPLAC, only circulating NK cells were present with no significant CD103 expression (**Fig. 2D**). NK cells from the mBlood were mostly CD16$^+$, while their tissue counterparts were CD16$^-$ in line with previously reported phenotypes.[6,40] We investigated whether CD16

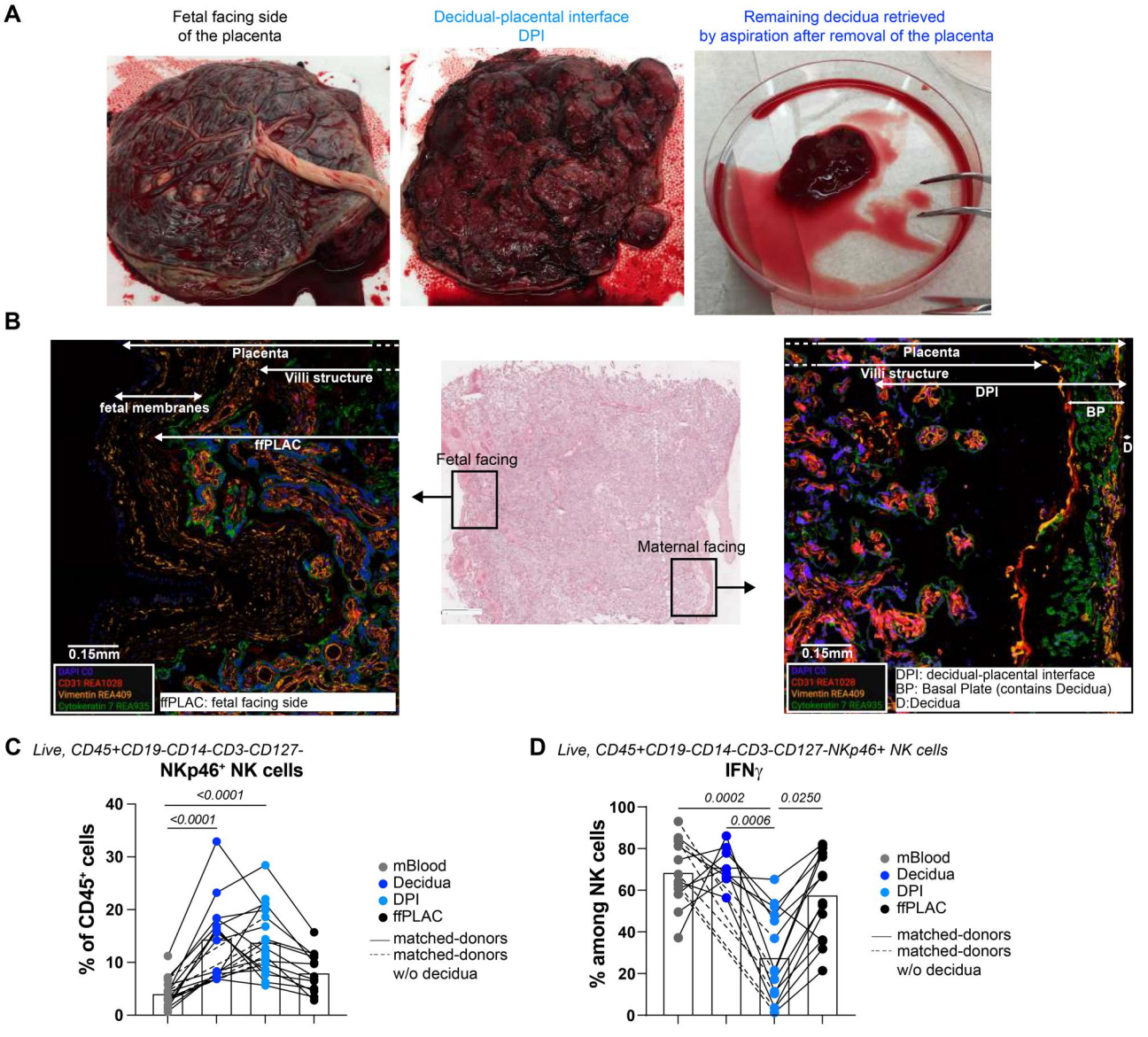

Figure 1. Functionally distinct decidual and decidual-placental interface NK cells. **(A)** Representative images of the two sides of the placenta and the aspirated decidua. (**B**) *(middle)* H&E image of a placenta section and respective 0.5 cm depth biopsies for each zone *(left)* fetal facing side, and *(right)* maternal facing side. Immunofluorescence images were generated using the MACSima^{TM} platform (the color of each marker is specified in the legend). (**C**) Frequency of NK cells in the different indicated tissues (mBlood n = 20, Decidua n = 15, DPI n = 20, ffPLAC n = 13). (**D**) After isolation, bulk single cells were stimulated for 24 h with IL-12, IL-15, and IL-18 (1nM each). GolgiPlug was added after 20hrs of culture. Graph showing IFN-γ expression among NK cells in the different indicated tissues (mBlood n = 14, Decidua n = 8, DPI n = 14, ffPLAC n = 14). Mean ± SD is shown for all graphs. Statistical analysis were performed using Kruskal–Wallis test with Dunn's multiple test comparisons.

expression might correlate with the lack of IFN-γ production in NK cells from the DPI. Again, we observed a decreased expression of IFN-γ both in CD16^{+} and CD16^{-} NK cells in the DPI compared to the Decidua, the mBlood and the ffPLAC (**Fig. 2E**).

Because we observed such a striking difference of ability to produce IFN-γ between the DPI and decidua but independent of CD103 or CD16 expression, we continued to further investigate whether this difference was associated with a distinct NK cell phenotype.

High parameter flow cytometry shows congruent phenotype between NK cells with different functionality

We compared the expression of residency, maturation, activation, activating and inhibitory receptors of NK cells in the different tissue sites using high parameter flow cytometry. We observed similar changes in expression in NK cells from the DPI and the decidua in comparison to NK cells from the mBlood and

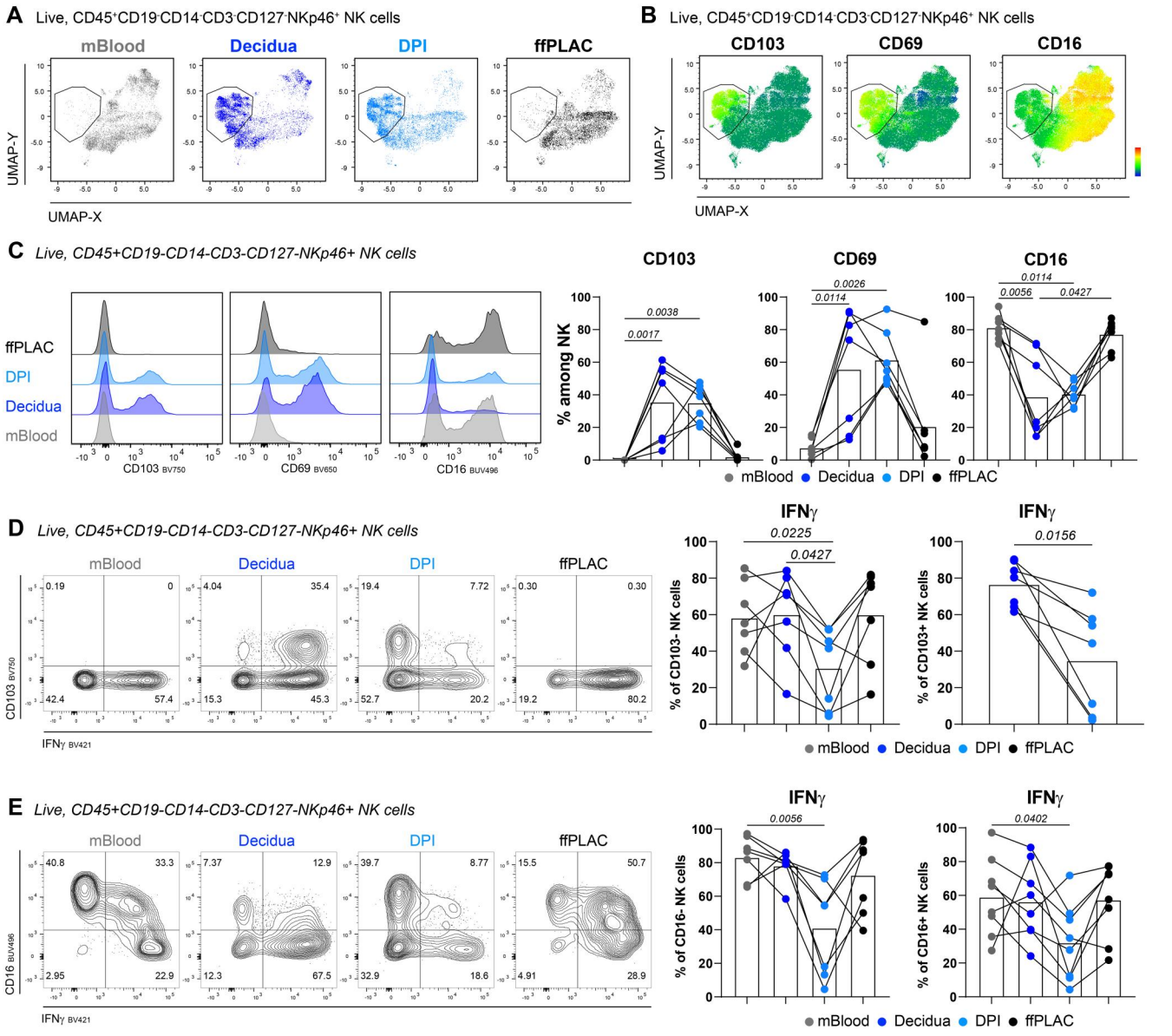

Figure 2. Functionally distinct resident NK cells. **(A–C)** After isolation, cells were stained using a 27-marker panel for flow cytometry (OMIP-070[32]) (**A**) NK cell phenotyping of 3 concatenated donors visualized by UMAP. (**B**) UMAP based on the expression of CD103, CD69, and CD16. Black gate identifies a cluster specific to Decidua and DPI NK cells. (**C**) *(left)* Histograms, and *(right)* quantification of indicated proteins (n = 7 matched donors). (**D–E**) After isolation, bulk single cells were stimulated for 24 h with IL-12, IL-15, and IL-18 (1 nM each). GolgiPlug was added after 20 h of culture. (**D**) *(left)* dot plots of IFN-γ and CD103 expression from 4 concatenated samples, and *(right)* graphs displaying IFN-γ expression among $CD103^-$ and $CD103^+$ NK cells (n = 7 matched donors). (**E**) *(left)* dot plots of IFN-γ and CD16 expression from 4 concatenated samples and *(right)* graphs displaying IFN-γ expression among $CD16^-$ and $CD16^+$ NK cells (n = 7 matched donors). Mean ± SD is shown for all graphs. Statistical analysis were performed using Friedman test with Dunn's multiple comparisons and (for E right) Wilcoxon test.

the ffPLAC (**Fig. 3A**). In particular, we observed a significant decrease of CX3CR1, CD11b, and CD2 in the DPI and the decidua compared to the mBlood. On the contrary, NK cells from the ffPLAC were very similar to the mBlood which indicates that these NK cells are likely circulating NK cells. CD38, whose expression has been reported to increase during pregnancy on NK cells,[66] was expressed at similar levels on NK cells across all tissue sites. Because $CD16^+$ and $CD16^-$ NK cell subsets display different phenotypes,[6,40] we also investigated changes in expression of the different markers among each population. Strikingly, we saw the same CD16-associated expression pattern of other biomarkers between NK cells from the decidua and the DPI compared to NK cells from mBlood or the ffPLAC (**Fig. 3B**). To further examine these NK cell population, we next analyzed the transcriptome of these NK cells.

RNA-sequencing shows congruent transcript between NK cells with different functionality

We isolated and sorted NK cells from the DPI, decidua, and mBlood (as a positive control for circulating NK cells) from 6

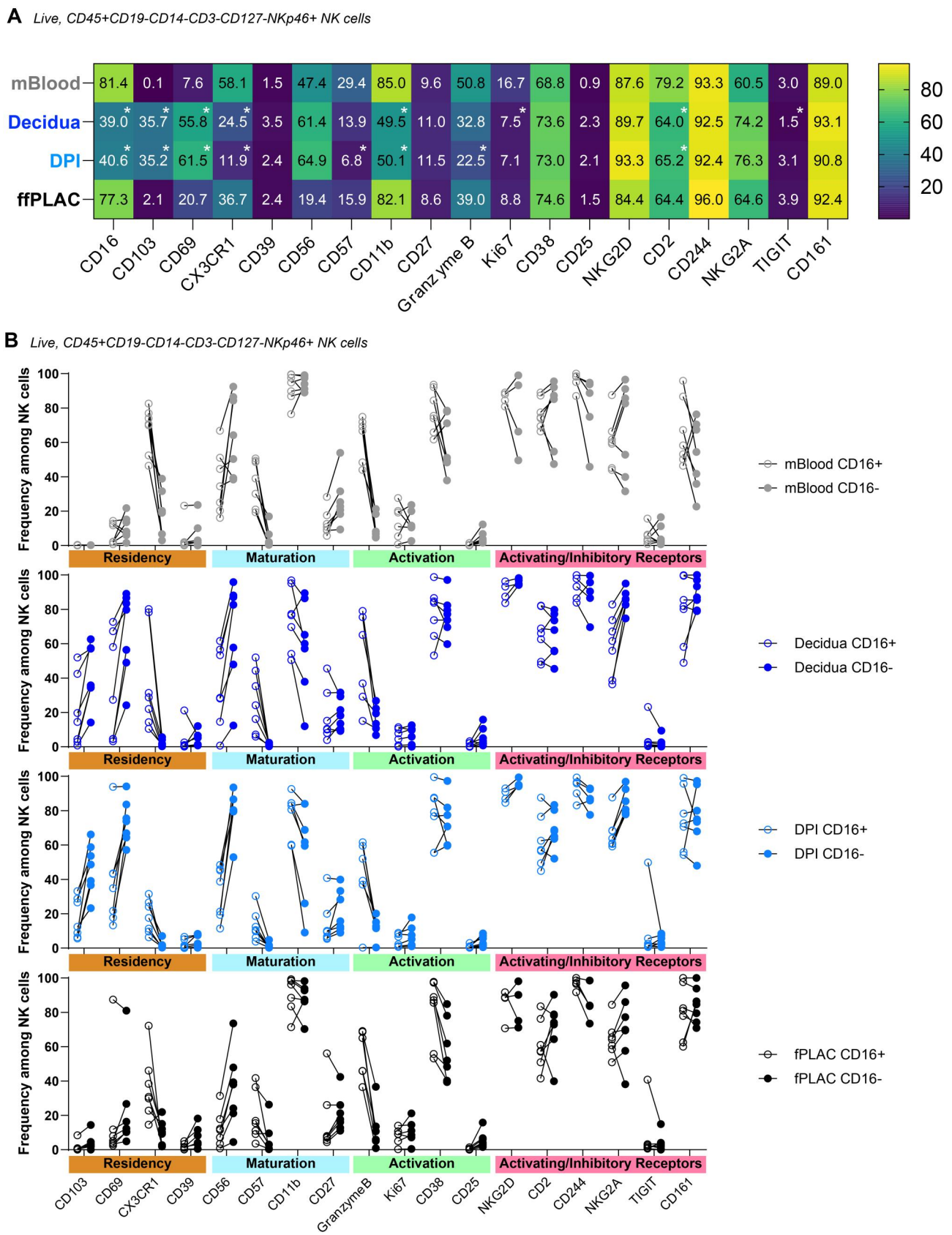

Figure 3. High parameter flow cytometry shows congruent phenotypes between decidual and decidual-placental interface NK cells. **(A)** Heatmaps representing the expression patterns for all the indicated proteins within the NK cells. Number inside the boxes represent the mean frequency for each marker among the specific subsets. Statistical analysis were performed using Friedman test with Dunn's multiple test comparisons. Asterisks inside the boxes indicate significant differences compared to the mBlood. **(B)** Expression of the different markers assessed by flow cytometry in the two main NK cell subsets across the four analyzed tissues (for A and B, *n* = 7 matched donors).

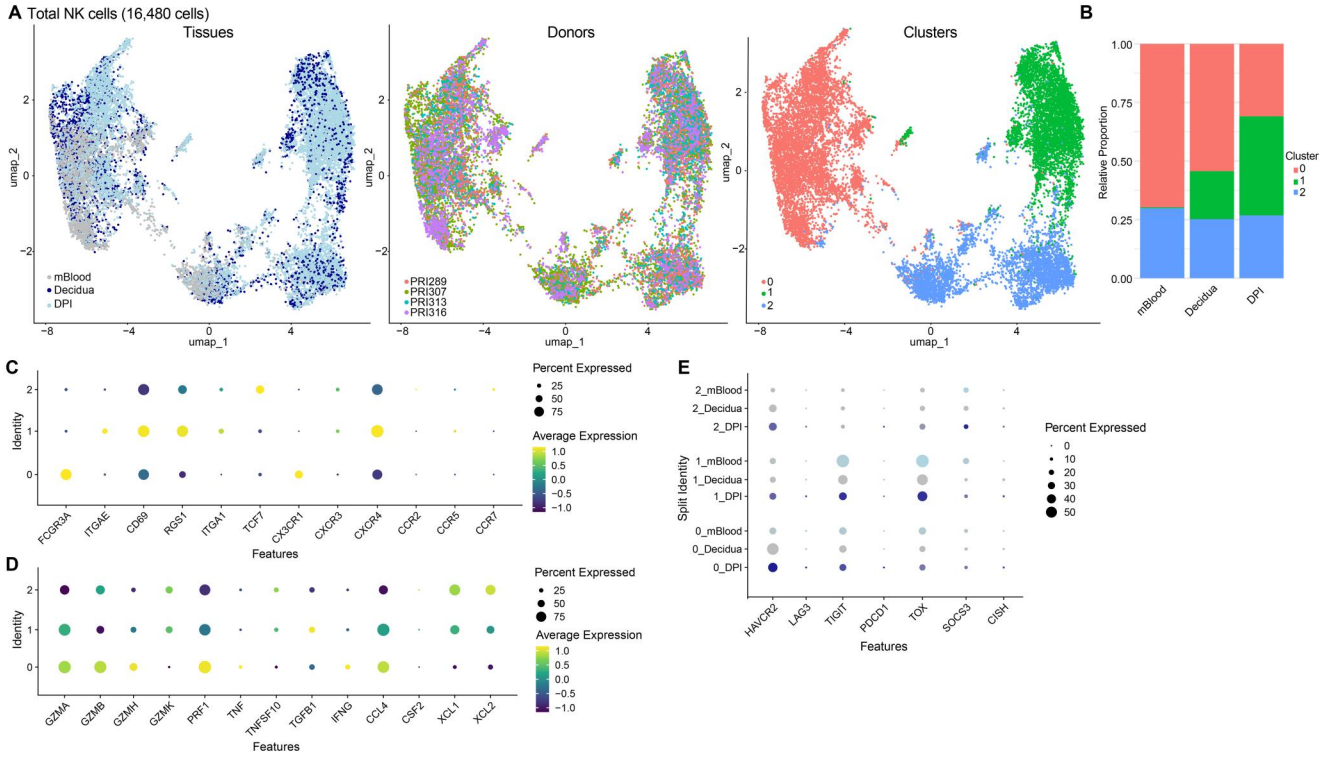

Figure 4. Congruent transcriptional profile between resident decidual and decidual-placental NK cells. **(A–B)** UMAP of the combined scRNA-seq data after quality filtering and Harmony integration, colored by *(left)* tissue origin, *(middle)* donor, and *(right)* cluster (resolution 0.1). (**B**) Cell proportion per cluster and sample type. **(C–E)** Scaled dot plot showing average transcript expression (color) and percent expression (dot size) of transcripts of (**C**) resident gene signatures, and (**D**) functional gene signature for each indicated cluster. (**E**) Scaled dot plot showing percent expression (dot size) of inhibition gene signature in indicated cluster for each tissue origin (color).

matched-donors and 2 additional donors for the DPI (all term placentas from unlabored C-sections) and processed 500 cells for RNAseq to assess similarities and differences in the transcript of NK cells in the different tissue sites. The sorted cell populations expressed both Tbet and Eomes consistent with an NK cell expression pattern (**Fig. S1B**). We observed 31 differentially expressed genes (DEG) between DPI and mBlood. Strikingly, yet consistent with our phenotypic profiling, we observed no DEG between NK cells from the decidua and the DPI (**Fig. S1C**). We then specifically compared the expression levels of genes associated with functional capacity and activation. We saw no differences between DPI and decidual NK cells for the transcript expression of IFNG, TNF, GNLY, GZMB, CD38, MKI67, or IL2RA (**Fig. S1D**).

We considered that single-cell resolution may be required to detect cells with transcriptional differences. For single-cell RNAseq experiments, we sorted pan CD45^{+} cells from the mBlood, DPI and decidua and enriched for NK cells during sorting. We were able to retrieve 16,480 NK cells from all tissue combined. Using a small resolution, we subsetted NK cells in 3 clusters. Clusters 0 and 2 were present in all tissues. Cluster 1 was almost exclusively present in the decidua and the DPI, distinguishing the "resident NK cell" population (**Fig. 4A and B**). Using AbSeq for combined protein and transcript profiling we also observed the expression of CD103 and the absence of CD16 at a protein level in cluster 1 confirming that these NK cells were resident NK cells (**Fig. S2A**). Moreover, confirming the bulk RNA sequencing results, these cells were bona fide NK cells according to their expression of Tbet and Eomes (**Fig. S2B**). At a transcript level, cluster 1 expressed higher levels of CD69, ITGAE, CXCR4 as well as RGS1 compared to cluster 0 and 2, confirming the presence of resident NK cells NK cells in both DPI and decidua (**Fig. 4C**). Clusters 0 and 2 were present in all 3 tissues mBlood, DPI and decidual NK cells and mirrored the transcriptional profile of circulating CD16^{+} NK cells and resident CD16^{-} NK cells respectively (**Fig. 4C and D**). Indeed, cluster 0 had increased expression of transcript of cytotoxic molecules (GZMA, GZMB, GZMH, IFNG, PRF1), while cluster 2 had increased expression of transcript involved in the recruitment of adaptive immune cells (XCL1, XCL2). As both resident and non-resident NK cells from the DPI had decreased ability to produce IFN-γ after stimulation, we wanted to compare the expression of molecules involved in the inhibition of NK cells for each tissue in each. We observed a small and equivalent level of transcript expression of LAG3, PDCD1, SOCS3, and CISH in all 3 clusters. HAVCR2 was increased in cluster 0 while TIGIT and TOX had increased expression level in cluster 1. However, comparable levels of HAVCR2, TIGIT and TOX transcripts were expressed in the 3 tissues (**Fig. 4E**). Finally, while single cell sequencing gave a deeper insight into NK cell transcript in the decidua and the DPI, neither NK cell transcriptome nor phenotype could predict this functional difference in the NK cell response in the DPI versus the decidua. These

results indicate that the functional properties are not necessarily predicted by biomarkers or gene expression signatures, and highlight the importance of ex vivo functional assays.

Discussion

Our study provides novel insights into the functional landscape of NK cells at the maternal-fetal interface in unlabored, full-term human pregnancies. Specifically, we demonstrate that NK cells from the full-term decidual-placental interface (DPI) are functionally less responsive than their decidual counterparts, exhibiting a markedly reduced capacity to produce IFN-γ in response to cytokine stimulation. Strikingly, this functional difference between tissue-adjacent NK cells could not be predicted by surface phenotype or transcriptional profiling.

NK cell tolerogenic properties are well described during the first trimester of pregnancy with reduced IFN-γ production [67] and cytotoxicity.[49,68] However, to what extent this decreased functionality of NK cells persist into term pregnancy has remained unresolved. Our findings suggest that functional dampening of NK cells persists in the DPI. Our observation that NK cells from the DPI are functionally distinct from their counterparts in the decidua—despite very similar phenotypic and transcriptional profiles—suggests that even high parameter flow cytometry and scRNAseq are not necessarily sufficient to predict ex vivo functional properties.

Tissue-derived signals could affect aspects of NK cell functionality without substantially altering the overall transcriptome. The role of the tissue microenvironment in shaping NK cell function is increasingly recognized. Tissue-resident NK cells (tr-NK) exhibit diverse phenotypes and functions depending on their location.[6,18] For instance, lung tr-NK cells have been shown to possess a unique profile of residency (with expression of CD49a and CD103) and to produce inflammatory cytokines upon stimulation.[63] Migration into tissues can also alter NK cell functionality as NK cells recirculating between blood and lungs have reduced cytotoxic abilities.[56] This idea is also supported by the recent work of Dean et al. who showed that NK cells recruited into tumors rapidly acquire tissue-resident phenotypes and lose effector function due to local environmental cues.[61] These phenotypic and transcriptomic differences between conventional NK cells and tissue resident NK cells has also been shown to be regulated by distinct cytokine cues (eg IL-21) and chromatin landscapes compared to circulating NK cells.[69] Moreover, Torcellan et al. further demonstrated that circulating conventional NK cells can convert into long-lived tr-NK cells following infection, acquiring enhanced recall capacity.[70] In line with these previous reports, we also observed distinct phenotypic and transcriptional changes between blood and tissue NK cells.

Importantly, our data show that the decreased ability of NK cells from the DPI was not restricted to just resident ($CD103^+$) NK cells, but also in non-resident DPI NK cells. The decrease in ex vivo responsiveness was furthermore not associated with increased expression of inhibitory markers such as PD-1, LAG-3, SOCS3, or TOX.

We considered that cytokines and metabolites present in the DPI may shape functional outcomes. Lipids for example, have been shown to mediate NK cell suppression in ovarian cancer ascites [71] and recent work implicates TGF-β and activin A as potent suppressors of NK cell function.[72] TGF-β is present in the syncytiotrophoblastic layer, chorionic plate, and the extravillous trophoblasts in the human term placenta.[73] It is unclear to which extent TGF-β availability varies between the DPI and the decidual tissue in our study. Future studies may be able to pinpoint cytokine and metabolite differences in DPI versus decidua. We also considered differences in oxygen concentration as a potential variable. Although we examined NK cell function at term, it is noteworthy that the placenta initially (during the 1^{st} trimester) develops in a hypoxic environment.[74] NK cell effector function typically decreases in hypoxic tissue environments[75] but is also associated with phenotypic changes such as a decrease in NKG2D expression.[75] However, we did not observe phenotypic changes or hypoxia-associated transcriptional changes. Overall, we favor the hypothesis that the plethora of environmental signals ultimately integrate to shape the functional properties of NK cells, akin to a model that we recently postulated for MAIT cells.[76] In our study, the functional adaptation of NK cells to this specific tissue environment (including proximity to fetal-derived trophoblasts) is reflected by a decrease in IFN-γ production following stimulation with pro-inflammatory cytokines. This could ensure that NK cells do not further amplify a pro-inflammatory response in an IFNγ-dependent manner[77] at the DPI thereby limiting the inflammatory response surrounding fetal trophoblasts.

We also acknowledge important experimental limitations: processes such as tissue digestion, cell sorting, cryopreservation or further ex vivo manipulation could alter NK cell properties. Thus, the observed effects may arise from both intrinsic and extrinsic factors. A related finding has been reported previously, where IFN-γ production by uterine NK cells was enhanced following stimulation with HLA-G, but only when the cells had been purified from total uterine mononuclear cell preparations.[78] Another limitation is that we did not analyze the full spectrum of KIR expression. NK cells are highly diverse at the single-cell level, owing to the combinatorial expression of activating and inhibitory receptors, and this diversity is closely tied to their functional potential.[79] By not capturing the entire breadth of KIR diversity, our study may therefore underestimate the full range of NK cell heterogeneity and its potential impact on tissue-specific function.

While our multi-modal approach (flow cytometry, single-cell transcriptomics) provides strong evidence for tissue site-specific functional differences, mechanistic insights underpinning these differences in NK cell responsiveness at the DPI are still uncertain. However, our findings highlight a previously underappreciated layer of functional ex vivo responsiveness among tissue-resident NK cells at the maternal-fetal interface despite similar phenotypes. Our data underscore the importance of the microanatomical context in shaping immune function during pregnancy and caution against exclusively relying on gene expression signatures to predict ex vivo functional properties.

Acknowledgments

The authors thank the Flow Cytometry Shared Resources Core of the FHCC, and the Genomics Shared Resources Core of the FHCC for sequencing. They thank Miltenyi Biotech for the

courtesy of the immunofluorescence images of the DPI based on the MACSima™ platform. They thank members of the Prlic lab for critical discussion.

Author contributions

Marie Frutoso (Conceptualization [Equal], Data curation [Lead], Formal analysis [Lead], Funding acquisition [Supporting], Investigation [Equal], Methodology [Lead], Project administration [Equal], Resources [Supporting], Software [Lead], Supervision [Supporting], Validation [Lead], Visualization [Lead], Writing—original draft [Lead], Writing—review & editing [Equal]), Caitlin S DeJong (Investigation [Equal], Writing—review & editing [Equal]), Raj Shree (Funding acquisition [Equal], Resources [Equal], Writing—review & editing [Equal]), Stephen A. McCartney (Investigation [Supporting], Resources [Lead], Writing—review & editing [Equal]), and Martin Prlic (Conceptualization [Equal], Data curation [Supporting], Formal analysis [Supporting], Funding acquisition [Lead], Investigation [Supporting], Methodology [Equal], Project administration [Equal], Resources [Lead], Software [Supporting], Supervision [Lead], Validation [Supporting], Visualization [Supporting], Writing—original draft [Supporting], Writing—review & editing [Equal])

Supplementary material

Supplementary material is available at *ImmunoHorizons* online.

Funding

This work was supported by National Institutes of Health (NIH) grants 1R01AI179712 and R21AI144677 (to M.P).

Conflicts of interest

This study has no conflict of interest.

Data availability

This work is the result of NIH funding, in whole or in part, and is subject to the NIH Public Access Policy. Through acceptance of this federal funding, the NIH has been given a right to make the work publicly available in PubMed Central. Sequencing data are available on GEO under access #GSE319493.

References

1. Vivier E, Tomasello E, Baratin M, Walzer T, Ugolini S. Functions of natural killer cells. Nat Immunol. 2008;9:503–510. https://doi.org/10.1038/ni1582.
2. Caligiuri MA. Human natural killer cells. Blood. 2008;112:461–469. https://doi.org/10.1182/blood-2007-09-077438.
3. Jonsson AH, Yokoyama WM. Natural killer cell tolerance licensing and other mechanisms. Adv Immunol. 2009;101:27–79. https://doi.org/10.1016/S0065-2776(08)01002-X.
4. Lanier LL. Evolutionary struggles between NK cells and viruses. Nat Rev Immunol. 2008;8:259–268. https://doi.org/10.1038/nri2276.
5. Di Santo JP. Natural killer cell developmental pathways: a question of balance. Annu Rev Immunol. 2006;24:257–286. https://doi.org/10.1146/annurev.immunol.24.021605.090700.
6. Dogra P et al. Tissue determinants of human NK cell development, function, and residence. Cell. 2020;180:749–763.e13. https://doi.org/10.1016/j.cell.2020.01.022.
7. Tang F et al. A pan-cancer single-cell panorama of human natural killer cells. Cell. 2023;186:4235–4251.e20. https://doi.org/10.1016/j.cell.2023.07.034.
8. Barry KC et al. A natural killer–dendritic cell axis defines checkpoint therapy–responsive tumor microenvironments. Nat Med. 2018;24:1178–1191. https://doi.org/10.1038/s41591-018-0085-8.
9. Ferlazzo G, Morandi B. Cross-talks between natural killer cells and distinct subsets of dendritic cells. Front Immunol. 2014;5:159. https://doi.org/10.3389/fimmu.2014.00159.
10. Schuster IS et al. Infection induces tissue-resident memory NK cells that safeguard tissue health. Immunity. 2023;56:531–546.e6. https://doi.org/10.1016/j.immuni.2023.01.016.
11. Schuster IS et al. TRAIL+ NK cells control CD4+ T cell responses during chronic viral infection to limit autoimmunity. Immunity. 2014;41:646–656. https://doi.org/10.1016/j.immuni.2014.09.013.
12. Andrews DM et al. Innate immunity defines the capacity of antiviral T cells to limit persistent infection. J Exp Med. 2010;207:1333–1343. https://doi.org/10.1084/jem.20091193.
13. Rydyznski C et al. Generation of cellular immune memory and B-cell immunity is impaired by natural killer cells. Nat Commun. 2015;6:6375. https://doi.org/10.1038/ncomms7375.
14. Rydyznski CE et al. Affinity maturation is impaired by natural killer cell suppression of germinal centers. Cell Rep. 2018;24:3367–3373.e4. https://doi.org/10.1016/j.celrep.2018.08.075.
15. De Maria A et al. Increased natural cytotoxicity receptor expression and relevant IL-10 production in NK cells from chronically infected viremic HCV patients. Eur J Immunol. 2007;37:445–455. https://doi.org/10.1002/eji.200635989.
16. Vivier E, Ugolini S. Regulatory natural killer cells: new players in the IL-10 anti-inflammatory response. Cell Host Microbe. 2009;6:493–495. https://doi.org/10.1016/j.chom.2009.12.001.
17. Erlebacher A. Immunology of the maternal-fetal interface. Annu Rev Immunol. 2013;31:387–411. https://doi.org/10.1146/annurev-immunol-032712-100003.
18. Le T, Reeves RK, McKinnon LR. The functional diversity of tissue-resident natural killer cells against infection. Immunology. 2022;167:28–39. https://doi.org/10.1111/imm.13523.
19. Moffett-King A. Natural killer cells and pregnancy. Nat Rev Immunol. 2002;2:656–663. https://doi.org/10.1038/nri886.
20. Hanna J et al. Decidual NK cells regulate key developmental processes at the human fetal-maternal interface. Nat Med. 2006;12:1065–1074. https://doi.org/10.1038/nm1452.
21. Siewiera J et al. Human cytomegalovirus infection elicits new decidual natural killer cell effector functions. PLoS Pathog. 2013;9:e1003257. https://doi.org/10.1371/journal.ppat.1003257.
22. De Mendonça Vieira R et al. Human term pregnancy decidual NK cells generate distinct cytotoxic responses. J Immunol. 2020;204:3149–3159. https://doi.org/10.4049/jimmunol.1901435.

23. Williams PJ, Searle RF, Robson SC, Innes BA, Bulmer JN. Decidual leucocyte populations in early to late gestation normal human pregnancy. J Reprod Immunol. 2009;82:24–31. https://doi.org/10.1016/j.jri.2009.08.001.
24. Sindram-Trujillo AP et al. Differential distribution of NK cells in decidua basalis compared with decidua parietalis after uncomplicated human term pregnancy. Hum Immunol. 2003;64:921–929. https://doi.org/10.1016/s0198-8859(03)00170-8.
25. Takahashi N et al. Factors associated with successful pregnancy in women of late reproductive age with uterine fibroids who undergo embryo cryopreservation before surgery. J Obstet Gynaecol Res. 2018;44:1956–1962. https://doi.org/10.1111/jog.13754.
26. Tilburgs T, Evans JH, Crespo ÂC, Strominger JL. The HLA-G cycle provides for both NK tolerance and immunity at the maternal-fetal interface. Proc Natl Acad Sci U S A. 2015;112:13312–13317. https://doi.org/10.1073/pnas.1517724112.
27. Hori T et al. Trophoblast stem cell-based organoid models of the human placental barrier. Nat Commun. 2024;15:962. https://doi.org/10.1038/s41467-024-45279-y.
28. Gude NM, Roberts CT, Kalionis B, King RG. Growth and function of the normal human placenta. Thromb Res. 2004;114:397–407. https://doi.org/10.1016/j.thromres.2004.06.038.
29. Spray ALP et al. Comparative analysis of immune cell populations from two sampling techniques of human term decidua utilizing high-parameter full-spectrum flow cytometry. Am J Reprod Immunol. 2025;94:e70130. https://doi.org/10.1111/aji.70130.
30. Mair F et al. Extricating human tumour immune alterations from tissue inflammation. Nature. 2022;605:728–735. https://doi.org/10.1038/s41586-022-04718-w.
31. Liechti T et al. An updated guide for the perplexed: cytometry in the high-dimensional era. Nat Immunol. 2021;22:1190–1197. https://doi.org/10.1038/s41590-021-01006-z.
32. Frutoso M, Mair F, Prlic M. OMIP-070: NKp46-based 27-color phenotyping to define natural killer cells isolated from human tumor tissues. Cytometry A. 2020;97:1052–1056. https://doi.org/10.1002/cyto.a.24230.
33. Perfetto SP, Ambrozak D, Nguyen R, Chattopadhyay PK, Roederer M. Quality assurance for polychromatic flow cytometry using a suite of calibration beads. Nat Protoc. 2012;7:2067–2079. https://doi.org/10.1038/nprot.2012.126.
34. Mair F, Tyznik AJ. High-dimensional immunophenotyping with fluorescence-based cytometry: a practical guidebook. Methods Mol Biol. 2019;2032:1–29. https://doi.org/10.1007/978-1-4939-9650-6_1.
35. Taber A, Konecny A, Oda SK, Scott-Browne J, Prlic M. TGF-β broadly modifies rather than specifically suppresses reactivated memory CD8 T cells in a dose-dependent manner. Proc Natl Acad Sci U S A. 2023;120:e2313228120. https://doi.org/10.1073/pnas.2313228120.
36. Butler A, Hoffman P, Smibert P, Papalexi E, Satija R. Integrating single-cell transcriptomic data across different conditions, technologies, and species. Nat Biotechnol. 2018;36:411–420. https://doi.org/10.1038/nbt.4096.
37. Korsunsky I et al. Fast, sensitive and accurate integration of single-cell data with Harmony. Nat Methods. 2019;16:1289–1296. https://doi.org/10.1038/s41592-019-0619-0.
38. Mair F et al. A targeted multi-omic analysis approach measures protein expression and low-abundance transcripts on the single-cell level. Cell Rep. 2020;31:107499. https://doi.org/10.1016/j.celrep.2020.03.063.
39. Finak G et al. MAST: a flexible statistical framework for assessing transcriptional changes and characterizing heterogeneity in single-cell RNA sequencing data. Genome Biol. 2015;16:278. https://doi.org/10.1186/s13059-015-0844-5.
40. Cooper MA, Fehniger TA, Caligiuri MA. The biology of human natural killer-cell subsets. Trends Immunol. 2001;22:633–640. https://doi.org/10.1016/s1471-4906(01)02060-9.
41. Cooper MA et al. Cytokine-induced memory-like natural killer cells. Proc Natl Acad Sci U S A. 2009;106:1915–1919. https://doi.org/10.1073/pnas.0813192106.
42. Romee R et al. Cytokine-induced memory-like natural killer cells exhibit enhanced responses against myeloid leukemia. Sci Transl Med. 2016;8:357ra123. https://doi.org/10.1126/scitranslmed.aaf2341.
43. Chaix J et al. Cutting edge: priming of NK cells by IL-18. J Immunol. 2008;181:1627–1631. https://doi.org/10.4049/jimmunol.181.3.1627.
44. Chan SH et al. Induction of interferon gamma production by natural killer cell stimulatory factor: characterization of the responder cells and synergy with other inducers. J Exp Med. 1991;173:869–879. https://doi.org/10.1084/jem.173.4.869.
45. Prlic M, Kamimura D, Bevan MJ. Rapid generation of a functional NK-cell compartment. Blood. 2007;110:2024–2026. https://doi.org/10.1182/blood-2007-04-086108.
46. Prlic M, Blazar BR, Farrar MA, Jameson SC. In vivo survival and homeostatic proliferation of natural killer cells. J Exp Med. 2003;197:967–976. https://doi.org/10.1084/jem.20021847.
47. Robertson MJ, Ritz J. Biology and clinical relevance of human natural killer cells. Blood. 1990;76:2421–2438. https://doi.org/10.1182/blood.V76.12.2421.2421
48. Kopcow HD et al. Human decidual NK cells form immature activating synapses and are not cytotoxic. Proc Natl Acad Sci U S A. 2005;102:15563–15568. https://doi.org/10.1073/pnas.0507835102.
49. Ritson A, Bulmer JN. Isolation and functional studies of granulated lymphocytes in first trimester human decidua. Clin Exp Immunol. 1989;77:263–268.
50. Rajagopalan S et al. Activation of NK cells by an endocytosed receptor for soluble HLA-G. PLoS Biol. 2006;4:e9. https://doi.org/10.1371/journal.pbio.0040009.
51. Long EO, Kim HS, Liu D, Peterson ME, Rajagopalan S. Controlling natural killer cell responses: integration of signals for activation and inhibition. Annu Rev Immunol. 2013;31:227–258. https://doi.org/10.1146/annurev-immunol-020711-075005.
52. Mackay LK et al. Cutting edge: CD69 interference with sphingosine-1-phosphate receptor function regulates peripheral T cell retention. J Immunol. 2015;194:2059–2063. https://doi.org/10.4049/jimmunol.1402256.
53. Freud AG et al. A human CD34(+) subset resides in lymph nodes and differentiates into CD56bright natural killer cells. Immunity. 2005;22:295–304. https://doi.org/10.1016/j.immuni.2005.01.013.
54. Gaynor LM, Colucci F. Uterine natural killer cells: functional distinctions and influence on pregnancy in humans and

mice. Front Immunol. 2017;8:467. https://doi.org/10.3389/fimmu.2017.00467.
55. Hudspeth K et al. Human liver-resident CD56(bright)/CD16(neg) NK cells are retained within hepatic sinusoids via the engagement of CCR5 and CXCR6 pathways. J Autoimmun. 2016;66:40–50. https://doi.org/10.1016/j.jaut.2015.08.011.
56. Marquardt N et al. Human lung natural killer cells are predominantly comprised of highly differentiated hypofunctional CD69-CD56dim cells. J Allergy Clin Immunol. 2017;139:1321–1330.e4. https://doi.org/10.1016/j.jaci.2016.07.043.
57. Melsen JE et al. Human bone marrow-resident natural killer cells have a unique transcriptional profile and resemble resident memory CD8+ T cells. Front Immunol. 2018;9:1829. https://doi.org/10.3389/fimmu.2018.01829.
58. Montaldo E et al. Unique Eomes(+) NK cell subsets are present in uterus and decidua during early pregnancy. Front Immunol. 2015;6:646. https://doi.org/10.3389/fimmu.2015.00646.
59. Lopez-Vergès S et al. CD57 defines a functionally distinct population of mature NK cells in the human CD56dimCD16+ NK-cell subset. Blood. 2010;116:3865–3874. https://doi.org/10.1182/blood-2010-04-282301.
60. Wilk AJ, Blish CA. Diversification of human NK cells: lessons from deep profiling. J Leukoc Biol. 2018;103:629–641. https://doi.org/10.1002/JLB.6RI0917-390R.
61. Dean I et al. Rapid functional impairment of natural killer cells following tumor entry limits anti-tumor immunity. Nat Commun. 2024;15:683. https://doi.org/10.1038/s41467-024-44789-z.
62. Brownlie D et al. Expansions of adaptive-like NK cells with a tissue-resident phenotype in human lung and blood. Proc Natl Acad Sci U S A. 2021;118:e2016580118. https://doi.org/10.1073/pnas.2016580118.
63. Marquardt N et al. Unique transcriptional and protein-expression signature in human lung tissue-resident NK cells. Nat Commun. 2019;10:3841. https://doi.org/10.1038/s41467-019-11632-9.
64. Degos C et al. Endometrial tumor microenvironment alters human NK cell recruitment, and resident NK cell phenotype and function. Front Immunol. 2019;10:877. https://doi.org/10.3389/fimmu.2019.00877.
65. Hegewisch-Solloa E et al. Mapping human natural killer cell development in pediatric tonsil by imaging mass cytometry and high-resolution microscopy. bioRxiv 2023;bioRxiv. 2023.09.05.556371. https://doi.org/10.1101/2023.09.05.556371.
66. Le Gars M et al. Pregnancy-induced alterations in NK cell phenotype and function. Front Immunol. 2019;10:2469. https://doi.org/10.3389/fimmu.2019.02469.
67. Saito S et al. Cytokine production by CD16-CD56 bright natural killer cells in the human early pregnancy decidua. Int Immunol. 1993;5:559–563. https://doi.org/10.1093/intimm/5.5.559.
68. Ferry BL et al. Cell populations in the human early pregnancy decidua: natural killer activity and response to interleukin-2 of CD56-positive large granular lymphocytes. Immunology. 1990;70:446–452.
69. Hu L et al. Genetic distinction between functional tissue-resident and conventional natural killer cells. iScience. 2023;26:107187. https://doi.org/10.1016/j.isci.2023.107187.
70. Torcellan T et al. Circulating NK cells establish tissue residency upon acute infection of skin and mediate accelerated effector responses to secondary infection. Immunity. 2024;57:124–140.e7. https://doi.org/10.1016/j.immuni.2023.11.018.
71. Slattery K et al. Uptake of lipids from ascites drives NK cell metabolic dysfunction in ovarian cancer. Sci Immunol. 2025;10:1–17. https://doi.org/10.1126/sciimmunol.adr4795
72. Rea A et al. Enhancing human NK cell antitumor function by knocking out SMAD4 to counteract TGFβ and activin A suppression. Nat Immunol. 2025;26:582–594. https://doi.org/10.1038/s41590-025-02103-z.
73. Schilling B, Yeh J. Transforming growth factor-beta(1), -beta(2), -beta(3) and their type I and II receptors in human term placenta. Gynecol Obstet Invest. 2000;50:19–23. https://doi.org/10.1159/000010272.
74. Patel J, Landers K, Mortimer RH, Richard K. Regulation of hypoxia inducible factors (HIF) in hypoxia and normoxia during placental development. Placenta. 2010;31:951–957. https://doi.org/10.1016/j.placenta.2010.08.008.
75. Chang T-D et al. Adaptation of natural killer cells to hypoxia: a review of the transcriptional, translational, and metabolic processes. Immunotargets Ther. 2025;14:99–121. https://doi.org/10.2147/ITT.S492334.
76. Konecny AJ, Huang Y, Setty M, Prlic M. Signals that control MAIT cell function in healthy and inflamed human tissues. Immunol Rev. 2024;323:138–149. https://doi.org/10.1111/imr.13325.
77. Schenkel JM, Fraser KA, Vezys V, Masopust D. Sensing and alarm function of resident memory $CD8^+$ T cells. Nat Immunol. 2013;14:509–513. https://doi.org/10.1038/ni.2568.
78. van der Meer A et al. Membrane-bound HLA-G activates proliferation and interferon- production by uterine natural killer cells. Mol Hum Reprod. 2004;10:189–195. https://doi.org/10.1093/molehr/gah032.
79. Horowitz A et al. Genetic and environmental determinants of human NK cell diversity revealed by mass cytometry. Sci Transl Med. 2013;5:208ra145. https://doi.org/10.1126/scitranslmed.3006702.